Polar Research

RESEARCH ARTICLE

Drivers, detection and impacts of rain-on-snow events on Banks Island, Canadian Arctic Archipelago: insights from remote sensing and Inuit Knowledge

Josée-Anne Langlois,[1,2] Alexandre Langlois,[1,2] Caroline Dolant,[1] Sachs Harbour Hunters & Trappers Committee, Resolute Bay Hunters & Trappers Association, Iviq Hunters & Trappers Association, Taloyoak Umaruliririgut Association & Cheryl Ann Johnson[1,3]

[1]Groupe de Recherche Interdisciplinaire sur les Milieux Polaires, Applied Geomatics Department, Sherbrooke University, Sherbrooke, QC, Canada; [2]Center for Northern Studies, Laval University, Quebec, QC, Canada; [3]Landscape Science & Technology, Environment and Climate Change Canada, Ottawa, ON, Canada

Abstract

Current warming trends in polar regions have increased the frequency of rain-on-snow (ROS), which impacts snow microstructure and leads to the formation of ice crusts. We draw on Inuit Knowledge (IQ), alongside passive microwave satellite imagery and local measurements, to investigate both the drivers and the consequences of ROS events on foraging conditions for Peary caribou (*Rangifer tarandus pearyi*) on Banks Island in the Canadian Arctic Archipelago. Our approach improved the detection of large-scale ROS events, and the remote sensing detection algorithm combined with IK revealed a significant increasing trend over time in the area affected by ROS on Banks Island during the fall from 1987 to 2023. Satellite imagery and IQ both indicated that the occurrence of ROS is higher in coastal areas of Banks Island. We demonstrated that both the presence of atmospheric rivers and the reduction of local sea ice in the fall are associated with an increase in the occurrence and intensity of ROS on Banks Island. Our article highlights how the complementarity among IQ, remote sensing, climate reanalysis models and local observations from weather stations can advance our understanding of ROS events and their impacts on wildlife. Identifying drivers of ROS is key to anticipating future effects on wildlife and the communities that depend on them. The approaches presented in this article show promising avenues for addressing these complex questions.

To access the supplementary material, please visit the article landing page

Keywords

Passive microwave; *Rangifer tarandus*; Inuit Qaujimajatuqangit; Indigenous Knowledge; atmospheric river; climate change

Correspondence

Josée-Anne Langlois, Applied Geomatics Department, Sherbrooke University, 2500 Bd de l'Université, J1K 2R1 Sherbrooke, QC, Canada. E-mail: josee-anne.langlois@usherbrooke.ca

Abbreviations

AO: Arctic Oscillation
AR: atmospheric river
CAA: Canadian Arctic Archipelago
DBSCAN: Density-Based Spatial Clustering of Applications with Noise
ERA5: European Centre for Medium-Range Weather Forecasts Atmospheric Reanalysis version 5 data set
FN: false negative
GRP: polarized gradient ratio
IMS: Interactive Multisensor Snow and Ice Mapping System (U.S. National Ice Center software package)
IQ: Inuit Knowledge
NAO: North Atlantic Oscillation
NARR: North American Regional Reanalysis data set
NOAA: National Oceanic and Atmospheric Administration (USA)
PMW: passive microwave
PNA: Pacific/North American Pattern
PWAT: precipitable water
ROS: rain-on-snow
SSM/I: Special Sensor Microwave Imager
SSMIS: Special Sensor Microwave Imager/Sounder
TN: true negative
TP: true positive
TB: brightness temperature

Introduction

Climate change and climate variability are affecting human health and well-being globally, with impacts that are most pronounced in the Arctic. The Arctic has warmed three to four times faster than the global average since 1979 because of Arctic amplification (Rantanen et al. 2022). This phenomenon is linked, among other factors,

Citation: *Polar Research* 2026, *45*, 12930, http://dx.doi.org/10.33265/polar.v45.12930

to reductions in sea ice and snow cover, which decrease surface albedo by exposing darker surfaces, creating positive feedback. Changes in atmospheric and oceanic circulation, as well as in cloud cover, also contribute to this positive feedback and further accelerate Arctic warming (Serreze & Barry 2011). Many studies project future increases in precipitation and rainfall in the Arctic (Walsh et al. 2020; Mooney & Li 2021; Serreze et al. 2021). Accurate spatial and temporal detection of ROS events in the Arctic remains challenging and limits our ability to detect trends in the occurrence of these events (Serreze et al. 2021).

ROS events can create ice layers within the snowpack that prevent herbivores from foraging. The formation of an ice layer in the snowpack in fall and early winter can increase energetic costs for large ungulates and, in the most severe cases, prevent them from accessing forage throughout the winter (Miller & Gunn 2003; Johnson et al. 2016). ROS events have led to massive die-offs of caribou and reindeer (*Rangifer tarandus*; Miller & Gunn 2003; Rennert et al. 2009; Forbes et al. 2016; Kaluskar et al. 2020). Less severe ROS events are also associated with poor body condition and low reproductive rates (Bartsch et al. 2010; Mallory & Boyce 2018). However, the ultimate impact of ROS on ungulate population persistence remains unclear. Some studies of reindeer (*R. t. platyrhynchus*), in the Norwegian Arctic archipelago of Svalbard, suggest that the impacts of ROS are density-dependent and may help stabilize population dynamics (Hansen et al. 2019; Loe et al. 2021). In contrast, Peary caribou (*R. t. pearyi*) in the CAA were listed as Endangered under Canada's Species at Risk Act in 2011 following a decline of > 35% over three generations, attributed to a series of extreme weather events (COSEPAC 2015; Johnson et al. 2016). Having increased in abundance, Peary caribou are now listed as Threatened (COSEPAC 2015).

Understanding the drivers of ROS is crucial for predicting their future occurrence and for anticipating and mitigating their impacts on Arctic ecosystems and Indigenous Peoples, whose customs, lifestyles, health and laws are closely tied to the land and sea across the region (Taylor 2005). The factors governing the occurrence and intensity of ROS are still poorly understood, and the lack of methods for detecting ROS events in the CAA remains an overarching challenge (Serreze et al. 2021). The low density of weather stations across the CAA makes it difficult to detect ROS events, which are often spatially localized (Rennert et al. 2009; Serreze et al. 2021).

Indigenous Knowledge can help guide research on ROS and its impacts on wildlife. The Arctic Council's definition of Indigenous Knowledge is relevant for this study: "a systematic way of thinking and knowing that is elaborated and applied to phenomena across biological, physical, cultural and linguistic systems" (Arctic Council Indigenous Peoples' Secretariat 2018). Furthermore, "It is a body of knowledge generated through cultural practices, lived experiences including extensive and multigenerational observations, lessons and skills" (Arctic Council Indigenous Peoples' Secretariat 2018). Studies with Sámi reindeer herders highlight the value of bridging Western science and Indigenous Knowledge to provide a more complete understanding of the effects of climate and weather on reindeer ecology (Eira et al. 2013; Markkula et al. 2019). Laptander (2023) worked with the Yamal Nenets people to understand how climate change affects their lives and reindeer herding activities. In the Canadian Arctic, the bridging of Western science and IQ has improved our understanding of wildlife health (Tomaselli et al. 2018), the consequences of changes in sea ice on caribou (Laidler et al. 2010; Paquette et al. 2023) and the impacts of climate change in the Arctic (Riedlinger 2001; Jolly et al. 2002; Pearce et al. 2009; Nancarrow & Chan 2010; Johnson et al. 2016).

The braiding of IQ with satellite remote sensing offers an avenue for detecting and analysing ROS events (Langlois et al. 2017; Serreze et al. 2021). PMW sensors and radar (active sensors) are both sensitive to the presence of liquid water in the snowpack. Radar sensors offer better spatial resolution than PMW sensors and have been successfully used to detect ROS events in Svalbard (Vickers et al. 2022). Bartsch et al. (2010, 2023) combined active and passive radar sensors to detect ROS and snowmelt events across the circumpolar Arctic. Dolant et al. (2016) developed an ROS detection algorithm on the basis of a PMW approach using 19 and 37 GHz in vertical and horizontal polarization. This method measures the signal reversal between the two frequencies caused by changes in the dielectric properties of the snow cover when liquid water accumulates on the snow surface. Sasseville et al. (2024) used this algorithm to generate ROS detection maps for the CAA at a spatial resolution of 3.125 km and detected a non-significant increase in ROS events per year across the CAA from 1987 to 2019.

Increased precipitation in the Arctic has two possible sources: an increase in local surface evaporation or an intensification of moisture transport from more distant regions (Bintanja 2018). ROS events in the Arctic are generally linked to the presence of extratropical cyclones, followed by a rapid drop in temperature that leads to ice formation within the snow cover (Hansen et al. 2014). ARs, defined as long bands of strong horizontal water vapour transport in the lower troposphere (Mo 2024), have been associated with major ROS events in the Arctic (Serreze et al. 2022). Rennert et al. (2009) identified positive air temperatures as one of the main factors contributing to an increase in ROS frequency. According to

Citation: *Polar Research* 2026, *45*, 12930, http://dx.doi.org/10.33265/polar.v45.12930

that study, local factors influencing surface evaporation appear to predominate over circulation changes, although both types of factors contribute to the frequency of ROS events in the Arctic (Rennert et al. 2009). The observed decrease in sea-ice extent in the Arctic Ocean results in changes in ocean–atmosphere interactions (Meier et al. 2022). These changes contribute to Arctic amplification by influencing surface albedo and may also affect ROS events by increasing surface evaporation (Forbes et al. 2016; Wickström et al. 2020).

In this study, we bring together IQ and remote sensing to detect and study ROS events on Banks Island in the CAA. More specifically, we (1) document the detection of large-scale ROS events in the Canadian Arctic on the basis of both IQ and PMW remote sensing techniques; (2) characterize the intensity of ROS events in terms of their spatial and temporal extent as a means of better quantifying the potential impacts of ROS on large herbivores; and (3) analyse correlations with AR and sea-ice concentration to investigate the drivers of large-scale ROS events in the CAA.

Methods

The methods used in this work are described in a methodological workflow diagrammed in Supplementary Fig. S1, along with details of all the data sets used (Supplementary Table S2).

Study area

Banks Island, in the western CAA, has an area of 70 028 km^2. The island is part of the Inuvialuit Settlement Region within the Northwest Territories of Canada. Banks Island is described as a polar desert influenced by Pacific air masses (Maxwell 1981). The landscape is composed of Arctic tundra and is dominated by flatlands (Johnson et al. 2016). Sachs Harbour, or Ikaahuk ("place where one crosses"), is the only settlement on Banks Island and is inhabited by 118 people, mostly Inuit (NWT Bureau of Statistics 2024). The island is home to muskoxen (*Ovibos moschatus*) and Peary caribou, among other wildlife species. People from Ikaahuk hunt caribou and muskoxen and this activity contributes significantly to the well-being of the community (Laidler & Grimwood 2010; Ljubicic et al. 2016). Hunting, harvesting and other land-based activities remain important for the community, contribute to subsistence and support the renewal of IQ and values (Riedlinger 2001; Ljubicic et al. 2022; Paquette et al. 2023).

Banks Island was chosen as the study site because of its relatively small size compared to neighbouring Victoria Island makes it more difficult for caribou and muskoxen to find unaffected habitats during freezing rain events (Riedlinger 2001). There are also three active weather stations managed by Environment and Climate Change Canada on Banks Island, providing local weather observations to validate ROS events detected using PMW imagery. The stations included are Sachs Harbour (71.99°N, 125.25°W), Thomsen River (73.23°N, 119.54°W) and Nangmagvik Lake (74.17°N, 119.99°W; Fig. 1). The Thomsen River and Nangmagvik Lake stations are in Aulavik National Park.

Inuit Knowledge

Hunters and Trappers from Ikaahuk have reported their observations of ROS events and major wildlife die-offs through various projects. For this study, we rely on IQ that has been shared and documented by Johnson et al. (2016), Riedlinger (2001) and SARC (2012). Additional information on ROS was also shared during workshops and interviews conducted between 2020 and 2024 as part of a multiyear research initiative aimed at identifying critical terrestrial habitat for Peary caribou. This project was initiated in 2019 to address the need to identify habitats on land required for species persistence in a federal Recovery Strategy (Environment and Climate Change Canada 2022). Workshops and interviews were conducted with Inuit partners from nine different communities: Tuktoyaktuk, Ulukhaktok, Paulatuk, Kugaaruk, Taloyoak, Aujuittuq (Grise Fiord), Ikaahuk (Sachs Harbour), Qausuittuq (Resolute Bay) and Iqaluktuuttiaq (Cambridge Bay). Hunters and Trappers Associations and Committees helped to identify knowledge-holders to participate in semi-directed interviews. Workshop activities included, but were not limited to, participatory mapping, fuzzy cognitive mapping and proportional piling. A total of 19 workshops and interviews were conducted, involving 117 participants. Of these workshops, five provided IQ that was included in this work (Supplementary Table S1). One workshop specifically focused on ROS and its consequences for caribou; participants were asked about past ROS events, their intensity, their impacts on caribou, and whether the frequency or intensity of ROS has changed over time (ICBPCP 2023). Two workshops focused on the effect of snow conditions on caribou, with specific questions related to ice layers within the snowpack (AGFPCP 2024; QRBPCP 2024). Timing of ROS events and their impacts on caribou were also shared during two additional workshops (ISHPCP 2022, 2023), although ROS was not the primary focus.

With participants' consent, workshops and interviews were audio-recorded. Audio recordings were transcribed

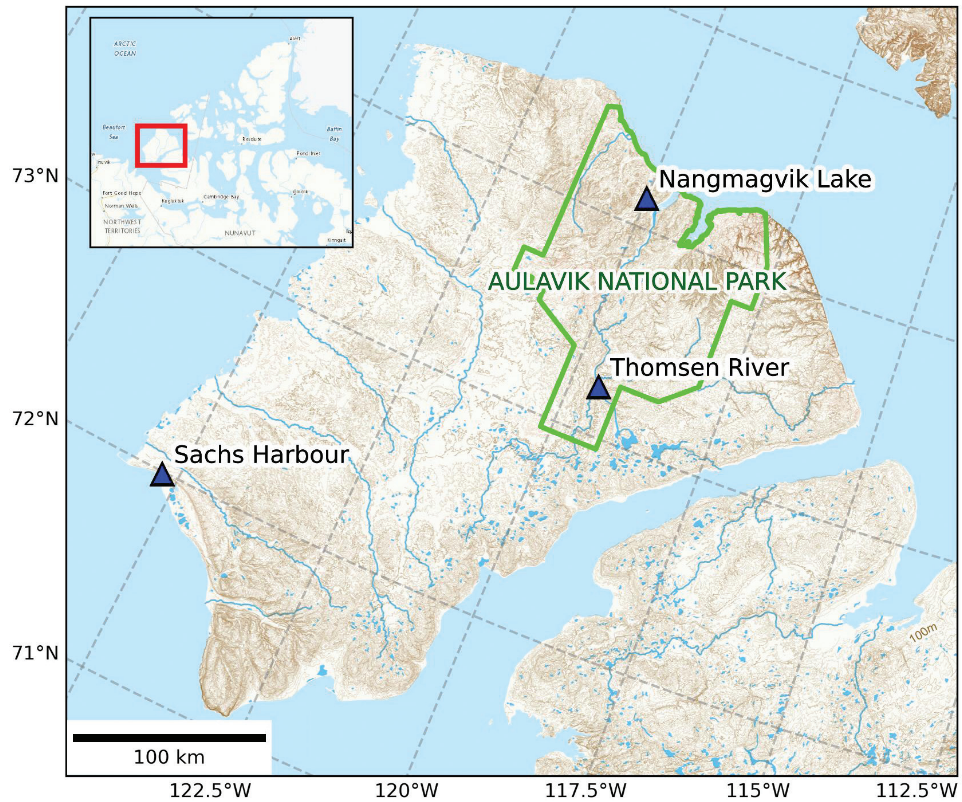

Fig. 1 Location of the weather stations on Banks Island (triangles). The green line represents the boundaries of Aulavik National Park of Canada (Natural Resources Canada 2016b). Basemap data are from Natural Resources Canada (2014, 2016a, 2024).

and thematically coded using Atlas.ti software into broad topics, including wildlife observations, disturbances and environmental changes. Transcript segments referring to ROS events and their consequences were coded under the theme "ROS." All citations coded as ROS were extracted, summarized and used to inform this study. In total, IQ from members of four communities— Ikaahuk, Taloyoak, Aujuittuq and Qausuittuq—was included in this work. Results on ROS were presented to and reviewed by the Hunters and Trappers Associations and Committees of these four communities. When possible, results were also discussed with individual participants who shared the IQ, to ensure proper interpretation and representation of IQ and to seek consent with its publication (AGFPCP 2025; ISHPCP 2025; QRBPCP 2025). Participants were also asked whether they wished to be named in the acknowledgements.

Research permits and ethical approval for the workshops and interviews were provided by the Nunavut Research Institute (no. 04 025 22N-M, no. 04 003 23R-M, no. 04 002 24R-M, no. 04 001 25R-M), the Aurora Research Institute (no. 16982, no. 17167, no. 17440, no. 17653), the University of Sherbrooke (no. 2023-3761) and McGill University (no. 21-08-021).

PMW ROS detection

We adapted the algorithm developed by Dolant et al. (2016) to detect ROS using the GRP (Eqn. 6). The algorithm detects the accumulation of liquid water at the surface of the snowpack during an ROS event. This accumulation leads to a strong dielectric contrast between the upper layers and the lower layers of the snowpack, resulting in an increase in emission at both 19 and 37 GHz frequencies (with a stronger increase at 37 GHz). This leads to higher TBs at 37 GHz than at 19 GHz in the horizontal polarization (Dolant et al. 2016; Sasseville et al. 2024). In this article, TB values were extracted from the MEaSUREs Calibrated Enhanced-Resolution Passive Microwave Daily data set (Brodzik et al. 2016) using a combination of sensors to cover the period from 1987 to 2023 (Table 1). This database consolidates 47 years of PMW measurements from various sensors into a coherent time series of TB values (Brodzik & Long 2018). The spatial resolution of the data set is 3.125 × 3.125 km for 37 GHz and 6.25 × 6.25 km for 19 GHz. We used the nearest-neighbour algorithm to resample the 19 GHz to 3.125 km. The satellite data set covers most of the Northern Hemisphere twice a day

Citation: *Polar Research* 2026, *45*, 12930, http://dx.doi.org/10.33265/polar.v45.12930

Table 1 List of sensors selected from the MEaSUREs database to detect ROS events.

Sensor	Platform	Start of the period	End of the period	Version
SSM/I	F08	7 Sep. 1987	15 Dec. 1991	1.3
	F11	16 Dec.1991	31 Aug. 1998	1.3
	F13	1 Sep. 1998	30 Apr. 2008	1.3
SSMIS	F17	1 Mar. 2008	31 Dec. 2015	1.3
	F18	1 Jan. 2016	31 Dec. 2023	1.3, 1.4, 1.5

(morning and evening passes). We applied the algorithm to detect ROS events from September to March, as most ROS events in the CAA occur in early autumn (Serreze et al. 2021).

The PMW data need to be corrected for atmospheric contributions, which are especially significant at 37 GHz, as demonstrated by Dolant et al. (2016). Atmospheric corrections were applied to the extracted TB values using the PWAT from NARR. These data are available at a spatial resolution of approximately 32 km for the entire study period (Mesinger et al. 2006). NARR data were reprojected and resampled to match the TB data set using the nearest-neighbour algorithm. This correction is based on the wave propagation model of Liebe (1989) implemented in the snow emission model developed at the Helsinki University of Technology (Pulliainen et al. 1999). We calculated atmospheric upwelling TB contributions ($TB_{\mathrm{atm}\uparrow}$) and atmospheric transmissivity for each frequency τ_f using the same parameters as those applied by Dolant et al. (2017) and Sasseville et al. (2024), derived from Roy et al. (2012), as follows:

$$TB_{\mathrm{atm}\uparrow(19)} = \left(0.879 \cdot PWAT\right) + 4.780 \qquad \text{Eqn. 1}$$

$$TB_{\mathrm{atm}\uparrow(37)} = \left(0.602 \cdot PWAT\right) + 18.297 \qquad \text{Eqn. 2}$$

$$\tau_{(19)} = \left(-0.003 \cdot PWAT\right) + 0.979 \qquad \text{Eqn. 3}$$

$$\tau_{(37)} = \left(-0.002 \cdot PWAT\right) + 0.924 \qquad \text{Eqn. 4}$$

The corrected TBs were obtained with this equation:

$$TB_{f\ \mathrm{corrected}}^{\mathrm{pol}} = TB_{f\ \mathrm{raw}}^{\mathrm{pol}} \cdot \tau_f + TB_{\mathrm{atm}\uparrow f} \qquad \text{Eqn. 5}$$

The GRP was calculated using corrected TB values. Previous studies applied a threshold of −10 on the GRP for ROS detection in the CAA (Dolant et al. 2017; Sasseville et al. 2024). In this study, we used a threshold of −2 in combination with a clustering algorithm to identify ROS events affecting a larger portion of the island and potentially having a greater negative impact on large herbivores. We tested different thresholds between 0 and −10 and −2 provided the best compromise in terms of TP and FN detections around weather stations.

$$\mathrm{GRP} = \frac{\dfrac{TB_{37}^{v} - TB_{19}^{v}}{TB_{37}^{v} + TB_{19}^{v}}}{\dfrac{TB_{37}^{h} - TB_{19}^{h}}{TB_{37}^{h} + TB_{19}^{h}}} \qquad \text{Eqn. 6}$$

Pixels were assigned a value of 1 if GRP was below −2 and 0 otherwise for all twice-daily images. The DBSCAN algorithm was applied to the binary images to retain groups of neighbouring pixels affected by ROS and to remove noise in the detection. DBSCAN detects clusters on the basis of density using two parameters (Ester et al. 1996): (1) Epsilon (ε), set at 8 km to represent the maximum distance between two neighbouring points; and (2) MinPts, set at 7 to represent the minimum number of pixels in a cluster, corresponding to a minimum cluster size of 90 to 250 km^2. On a single image, this clustering algorithm removed pixels or groups of pixels affected by ROS that were smaller than 250 km^2. The daily movement range of a sedentary Arctic caribou has been estimated at approximately 4 km^2 (Bergman et al. 2000). This movement rate is also consistent with the daily movement rate of collared Dolphin and Union caribou measured during staging, which was below 5 km day^{-1} (Leclerc & Boulanger 2018). Tews et al. (2007) used this daily range in their model for Peary caribou and estimated that an animal would die after 14 days of forage inaccessibility during winter. At an average movement rate of 2 km day^{-1}, an animal would require approximately 5 to 8 days to move out of an area of 250 km^2 if it moved in a relatively straight line. Thus, a ROS event that creates ice layers over an area of 100 to 250 km^2 would likely impact herbivores by limiting forage access over several days and by increasing their energetic costs on account of having to move out of the affected area.

The identified ROS occurrences were filtered to include only days with snow on the ground to avoid false positives (i.e., detection of ROS when no snow is present). We used the snow-cover database produced by NOAA, which provides weekly maps starting in 1966 and daily maps beginning in 1997 (Robinson et al. 2012). The maps produced between 1980 and 1997 were digitized at a spatial resolution of 24 km and accessible as the Rutgers Northern Hemisphere 24 km Weekly Snow Cover Extent data set (Robinson & Estilow 2021). From 1997 onward, there were daily IMS maps (Ramsay 1998) at a spatial resolution of 24 km and—from 2004—at 4 km (U.S.

National Ice Center 2008). These snow-cover maps are created using a combination of visible and PMW satellite imagery. We used the Rutgers Northern Hemisphere weekly snow-cover extent data set at 24 km resolution from 1987 to 1997, obtained from the National Snow and Ice Data Center (Robinson & Estilow 2021). We used the daily IMS snow-cover maps at 24 km resolution from 1997 to 2004 and at 4 km spatial resolution from 2004 onward. These daily snow-cover maps were obtained from the National Snow and Ice Data Center (U.S. National Ice Center 2008). All weekly and daily snow-cover maps were reprojected and resampled to match the GRP data set. When weekly snow-cover maps were used, snow cover was assumed to be present for the week preceding the date assigned to the map (Robinson & Estilow 2021). For each pixel where ROS was detected on the basis of the GRP, we retained only those for which snow-cover products indicated snow on the ground. This process was used to remove false detections of ROS and retain only events occurring when there was snow on the ground.

We used the same snow-cover data sets to calculate the number of days with snow cover on Banks Island for the months of September and October. For each year, we counted the number of days in September and October during which the snow-cover data sets indicated that at least 70% of the island was covered by snow. This information was used in the temporal trend analysis of ROS detection to account for interannual changes in the timing of snow onset in the fall.

Meteorological station observations of ROS

Of the three active weather stations on Banks Island, only the Sachs Harbour station is staffed and able to report precipitation and detailed atmospheric conditions. Meteorological data are available from 1955 onward for Sachs Harbour, from 1996 onward for the Nangmagvik Lake station and from 1997 onward for the Thomsen River station.

A ROS event was considered to have occurred at a weather station on the basis of thresholds of mean daily temperature and total daily precipitation (Wickström et al. 2020; Vickers et al. 2022). We used data from the Sachs Harbour weather station to compare daily total precipitation and mean daily temperature on days when a visual observer at the station identified rain or snow. There is a significant difference between daily mean temperatures recorded when rain was observed by station staff compared to when snow was observed, according to a Kolmogorov-Smirnov non-parametric test. This statistical test measures the distance D (ranging from 0 to 1) between two distributions. The distance between the distributions of daily mean temperatures when rain was observed (distribution 1) and when snow was observed (distribution 2) was moderately high and statistically significant ($D = 0.77, p < 10^{-60}$). The optimal threshold temperature separating the two cumulative distribution functions was −1.4 °C (Fig. 2). A precipitation threshold of 0.2 mm was used to define an ROS event based on the 5th percentile of total daily precipitation measured at the Sachs Harbour weather station during fall over the full study period (1987–2023). Both a daily mean temperature greater than or equal to −1.4 °C and a total daily precipitation greater than or equal to 0.20 mm were required to identify a local ROS event at the weather stations. At Sachs Harbour, a local ROS event was also identified when the observer reported rain or drizzle. These detections were used to validate ROS events detected using PMW algorithm.

Localized accuracy of ROS detection

Temperature and precipitation observations at the weather stations were used to validate the occurrence of ROS in the surrounding areas of the stations and to derive accuracy metrics for two local ROS detection algorithms on the basis of PMW imagery: (1) a first method using a GRP threshold of −10 for ROS detection (Sasseville et al. 2024); and (2) a second method involving the clustering of all GRP values below −2. A localized ROS event was considered to have occurred based on the PMW

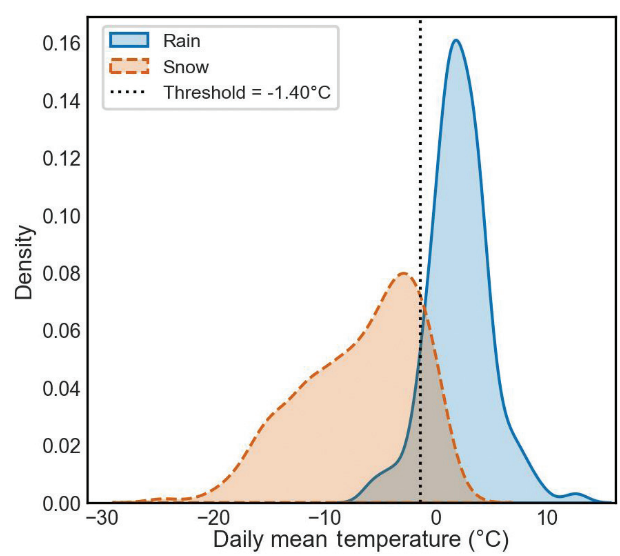

Fig. 2 Empirical cumulative distribution functions of daily mean temperature measured at the Sachs Harbour weather station when the observer identified rain or snow for the months of September and October between 1987 and 2023, when snow was on the ground.

algorithms only when it affected more than 5% of the pixels within a 10 km radius of a station in at least one of the two PMW images produced per day (morning and evening passes) and when snow-cover extent exceeded 70%.

A TP detection was counted when both the PMW algorithm and meteorological data detected a ROS event around a specific station on a given date. A false positive (FP) was counted when the PMW algorithm detected a ROS event that was not detected using local data. A FN was counted when the PMW algorithm did not detect a ROS event that was detected using local weather observations, and a TN was counted when neither source detected a ROS event on a given date. Local overall accuracy was derived from these metrics for each of the three weather stations (Eqn. 7).

$$\text{Accuracy} = \frac{(TP + TN)}{(TP + FP + TN + FN)} \qquad \text{Eqn. 7}$$

When the data are imbalanced, as is the case in this study because there are fewer days with ROS detection than days without ROS, it is preferable to use multiple accuracy metrics (Akosa 2017). We therefore calculated commission and omission errors, as well as the F1-score using the precision rate (TP/[TP+FP]) and the recall rate (TP/[TP+FN]).

$$\text{Commission error} = \frac{FP}{(TP + FP)} \qquad \text{Eqn. 8}$$

$$\text{Omission error} = \frac{FN}{(TP + FN)} \qquad \text{Eqn. 9}$$

$$F1\ \text{Score} = 2\ \text{X}\ \frac{(Precision\ rate * Recall\ rate)}{(Precision\ rate + Recall\ rate)} \qquad \text{Eqn. 10}$$

Detection of large-scale ROS events

From the daily detection of ROS using PMW imagery, we conducted further analyses to identify large-scale ROS events by identifying consecutive days with significant areas affected by ROS. We therefore identified dates when ROS was detected over 3.7% or more of the island (2537 km^2), corresponding to the 95th percentile of the daily area affected by ROS over the entire study period. Individual ROS events were then defined as consecutive days during which at least 2537 km^2 of the island was affected by ROS. ROS events separated by only one day were merged into a single event. Maps were created for each detected ROS events to identify the areas affected by ROS over the duration of each event.

To place the spatial extent threshold of ROS in the context of caribou ecology, 2537 corresponds to 20% of the winter range of Peary caribou on Banks Island, estimated at about 12 000 km^2 on the basis of the digitization of a map published by Larter & Nagy (1994). A ROS event was reported in October 1993, during which approximately 50% of the winter range of caribou was covered by ice (Larter & Nagy 1994). This icing event did not affect calf survival during the winter, but a reduction in the number of caribou calves was observed the following summer (Nagy et al. 2013).

Accuracy of large-scale ROS events

In contrast to the local accuracy calculated to validate the algorithm around each weather station, we used a similar, but different, approach to validate the detection of large-scale ROS events. A large-scale ROS event was considered a TP when it was identified through IQ or when at least one weather station detected a ROS event on at least one day of the event (i.e., daily mean temperature ≥ −1.4 °C and total daily precipitation ≥ 0.2 mm, or when rain or drizzle was reported at Sachs Harbour).

Intensity of large-scale ROS events

Three variables were used to characterize the intensity of each ROS event: the duration of the event (days), the total area affected by ROS (km^2), and the total amount of precipitation (mm). The duration of an event was calculated on the basis of the PMW ROS detection algorithm. Consecutive days with more than 3.7% of the island affected by ROS, as detected using PMW imagery, were considered part of a single event. The number of consecutive days meeting this 3.7% threshold was used as an indicator of event duration and, therefore, of intensity. The total area affected by each ROS event was calculated as a second intensity variable using the PMW ROS detection algorithm. Daily ROS maps derived from PMW were merged into a single raster over the duration of each event (i.e., consecutive days with more than 3.7% of the island affected by ROS). The total number of pixels affected by ROS at least once during the event was then counted and multiplied by the area of each pixel (3.125 km * 3.125 km = 9.77 km^2).

It was not possible to directly derive the total amount of precipitation associated with a ROS event from PMW data. We therefore used ERA5 precipitation (Mo 2024), based on the dates of ROS events detected with PMW. Total precipitation for each 6-hour time step (TP6H, mm) was averaged over Banks Island and summed over the duration of each ROS event.

The three intensity variables—total area affected by ROS, event duration and total precipitation—were normalized between 0 and 1 across all events. For each event, the three normalized indicators were averaged to calculate a composite intensity score ranging from 0 to 1, with values closer to 1 representing the most intense ROS events detected on Banks Island over the study period.

$$\text{Intensity score} = \frac{\text{Normalized area} + \text{Normalized duration} + \text{Normalized total precipitation}}{3}$$

Eqn. 11

Environmental and meteorological drivers of ROS events

ROS events in the Arctic can be influenced either by the remote transport of moisture, such as AR, or by local sources of evaporation, such as nearby open water. Correlation analyses were used to quantify relationships between AR occurrence, sea-ice anomalies and ROS events and their intensity. We used an ERA5-based data set specifically developed for AR detection (Mo 2024). This data set uses ERA5 variables to identify ARs at 6-hour intervals from 1940 to the present. Two different AR detection algorithms are implemented in this data_ set: tARget-v3 and mtARget-v3. Both rely on the geometry and intensity of integrated water vapour transport to identify ARs at a given time. The tARget-v3 algorithm is stricter with respect to the poleward direction of ARs, whereas the modified version (mtARget-v3) allows for the detection of ARs that change direction in extratropical regions. We used AR detections from both algorithms in this study. An AR was considered to have occurred when at least one of the algorithms detected an AR over Banks Island (covering 25% or more of the Island's area) for at least one time step during a ROS event. A Mann-Whitney U test was used to compare large-scale ROS event intensity scores, as well as individual intensity variables, with and without AR occurrence.

Weekly sea-ice charts from the Canadian Ice Service were used to assess the influence of sea-ice conditions on ROS events. We hypothesized that evaporation from open water surrounding Banks Island could increase the occurrence and intensity of ROS events (Forbes et al. 2016; Wickström et al. 2020). Weekly vector maps of total sea-ice concentration were rasterized at a resolution of 500 m × 500 m and averaged on a monthly basis (Government of Canada 2021). A climatological mean was calculated using the 1991–2010 reference period. Sea-ice concentration anomalies were calculated at the pixel level and subsequently averaged over all pixels within a 50 km buffer around Banks Island to obtain a single monthly anomaly index. Sea-ice anomalies were compared to the total area affected by ROS during the fall for each year using linear regression.

We also examined whether large-scale climate oscillation patterns were associated with interannual variability in the total area affected by ROS in the fall, given the influence of climate oscillations on precipitation (Putkonen & Roe 2003; Rennert et al. 2009). September and October indices for three climate patterns—the NAO, AO and PNA—were averaged and compared to the total area affected by ROS, normalized by the number of days with snow cover, the number of large-scale ROS events and the total duration of large-scale ROS events per fall, using Spearman's rank correlation coefficient.

Results

Inuit Knowledge of ROS

IQ about ROS was shared during workshops and interviews conducted in different communities across the Canadian Arctic in the context of the Peary Caribou Project. None of the workshops focused specifically on ROS, except for the workshop held in Iqaluktuuttiaq in 2023 (ICBPCP 2023). Nevertheless, ROS was frequently mentioned by participants at the workshops and was included in the thematic coding. The citations referring to rain and ROS were extracted from the thematically coded interview transcripts and summarized (Table 2). The IQ covers a wide range of topics related to ROS, including drivers, occurrence and consequences for wildlife. On Banks Island specifically, community members have observed an increase in the frequency of rain during late fall over the past 10 years (ISHPCP 2022). Most rain and humidity on Banks Island are perceived to have a coastal source, with moisture coming from the open ocean and not reaching inland areas, which are drier (ISHPCP 2023). Most mentions of rain and ROS are associated with the fall season.

We created a list of ROS and die-off events reported for caribou and muskoxen on Banks Island (SARC 2012; Johnson et al. 2016; ISHPCP 2023; Table 3). Events reported by community members were used to validate the large-scale ROS events detected using PMW imagery. It should be noted that no workshop was done specifically to compile a list of ROS events that have occurred on Banks Island. We therefore cannot assume that this is a comprehensive list of ROS events. However, we

Citation: *Polar Research* 2026, *45*, 12930, http://dx.doi.org/10.33265/polar.v45.12930

Table 2 A summary of IQ of ROS shared during workshops and interviews (Peary Caribou Project).

Summary	Source	Region concerned
More rain and melting snow in late fall for the last 10 years on Banks Island. Freezing rain is covering up food for caribou.	ISHPCP 2022	Banks
More rain and humidity about 10 miles closer to the ocean, and drier inland, with rain and humidity on the coast coming from the ocean.	ISHPCP 2023	Banks
The summers are longer now than in the 1970s, so animals can eat for longer, but in 2022 and 2023 it rained on the snow and it must make it hard for the animals to eat.	ISHPCP 2023	Banks
Moderate and heavy rain is a new phenomenon on Banks Island. Participants suggested that rain before freeze-up does more damage to wildlife by saturating the ground followed by freezing, and it also affects river debits in the spring as more water will flow to the river.	ICBPCP 2023	Banks
There was a ROS in November in the early or mid-1980s. The snow froze, and a participant suggested that many Peary caribou died at this time. They observed fewer Peary caribou after this event.	ICBPCP 2023	Boothia Peninsula
There was a ROS in the mid- to late 1980s in the High Arctic Islands, including Prince of Wales Island. There was enough snow to travel on, but a late rainfall completely wiped out the snow and the ground froze. A participant mentioned that biologist Anne Gunn later reported a big die-off of Peary caribou.	ICBPCP 2023	Boothia Peninsula, Prince of Wales Island
There was a ROS in December 2022 in Sachs Harbour, and a participant suggested it was mainly in coastal areas. It was harder to walk because the snow stayed soft after the rain.	ICBPCP 2023	Banks
When the bottom layer of snow (*pukaq*, ice crystal snow) is covered by harder snow or ice crust, it is harder for animals to smell the vegetation underneath the snow.	ICBPCP 2023	General
There were ROS events in the early 1990s on Somerset, Prince of Wales and Bathurst islands, and lots of caribou died.	QRBPCP 2024	Bathurst, Somerset, Prince of Wales
ROS for three consecutive years around or before 2000s on Bathurst Island may have resulted in low muskox and caribou numbers.	QRBPCP 2024	Bathurst
Before 2000, there was rain in the fall for three years in a row on Bathurst Islands, and there was a big die-off of muskox and caribou, with carcasses found by Parks Canada.	QRBPCP 2024	Bathurst
Rain or warm wind in October after the snow will harden the snow.	AGFPCP 2024	Aujuittuq
Many adult muskoxen and calves died after it rained in December in the 1990s.	AGFPCP 2024	Aujuittuq
In the fall of 2023, the snow melted and froze again, making the snow very hard, like pavement, and participant said it must be hard for the animals to dig through.	AGFPCP 2024	Aujuittuq
Caribou are on the higher ground, where it is colder and precipitation mostly falls as snow and not rain, while muskoxen eat mainly in the valley and are more affected by ROS at the beginning of the season.	AGFPCP 2024	Aujuittuq
Drizzle in the fall increases the hardness of the snow even if it does not create an ice layer.	QRBPCP 2024	Bathurst, Cornwallis

hypothesize that these events may represent the most impactful ROS events in terms of consequences for caribou, as the reports and workshops used to derive this list were all focused on Peary caribou.

Detection of ROS

We compared two versions of the ROS detection algorithms using PMW imagery: (1) the original version developed by Dolant et al. (2016, 2017) using a GRP threshold of −10; and (2) our proposed modification using a GRP threshold of −2 followed by a clustering algorithm. No ROS events were detected on Banks Island between December and March over the entire study period. The majority of ROS events were detected in September and October, with only two days of ROS detected in November, which were classified as false positives on the basis of local weather observations. Figure 3 shows the number of days with detected ROS affecting an area equal to or greater than 3.7% of the island for each year during the months of September and October.

The local accuracy metrics were calculated for the months of September and October at the three weather stations, as well as for the pooled data across all three sites (Table 4). While overall accuracy is slightly higher using the original method with a GRP threshold of -10, the F1-score is higher when using the adapted method with a GRP threshold of −2 combined with the clustering algorithm, except for the validation at the Thomsen River station, where the opposite trend is observed; however, this result is based on a limited number of ROS events. Commission errors are high but similar for both methods, indicating an overestimation of ROS events using PMW imagery for both approaches. In contrast, omission errors are reduced when using the clustering algorithm compared to the simple thresholding approach with GRP < −10.

Table 3 List of ROS events and die-off reported for Banks Island.

Date	Events	Peary caribou population event	Sources	Region affected
1987–88	Freezing rain	400 caribou deaths due to weather 1987–89	Nagy et al. 1996	Banks
1988–89	Freezing rain	400 caribou deaths due to weather 1987–89	Nagy et al. 1996	Banks, Victoria, Prince of Wales
1990–91	Freezing rain	60 caribou deaths due to weather	Nagy et al. 1996	Banks, Victoria, Prince of Wales
Oct. 1993	Inuvialuit hunters reported freezing rains during October 1993, covering ca. 50% of caribou winter range	Productivity was reduced; however, overwinter survival of calves for winter 1993–94 was high	Larter & Nagy 1994; Nagy & Gunn 2004; Nagy et al. 2013	Banks
Oct. 2003	An October icing event led to ground-fast ice, with ca. 47 000 km^2 covered by ice	No caribou die-off was associated with the icing event, but high muskox mortality. Lower calf productivity in 2004	Nagy & Gunn 2004; Gunn et al. 2006; Rennert et al. 2009; Nagy et al. 2013	Banks, Victoria
Fall 2022	A participant reported ROS	The participant mentioned it could have affected access to forage	ISHPCP 2023	Banks
Fall 2023	A participant reported ROS	The participant mentioned it could have affected access to forage	ISHPCP 2023	Banks

Twice-daily PMW images from 1987 to 2023 for the months of September and October were used to calculate the number of times ROS was detected for each pixel on Banks Island. A higher concentration of ROS occurrences was observed in coastal areas, while ROS events in the interior of the island were less frequent (Fig. 4). This result is consistent with IQ shared by community members, who reported that rain and humidity are more frequent within approximately 16 km of the coast on Banks Island (Table 2; Riedlinger 2001; ISHPCP 2023). This pattern is also consistent with previous studies reporting that coastal ROS events in the Arctic are more frequent than inland events (Rennert et al. 2009; Wilson et al. 2013; Serreze et al. 2021).

The daily area affected by ROS was summed for each year (September–October only) to analyse temporal trends. This metric represents the sum of daily ROS-affected areas, such that the same area may be counted multiple times within a given year if it was affected by ROS on multiple days. The summed ROS area could be influenced by the length of the snow season, with longer seasons contributing more to the annual total. We therefore standardized the summed ROS metric by dividing it by the number of days with snow cover on Banks Island for each year, based on NOAA snow-cover extent data sets. Only days with more than 70% snow cover over the whole Island were considered in the calculations. There is an increase in the area affected by ROS over time (Fig. 5), which is consistent with IQ indicating that rain in the fall

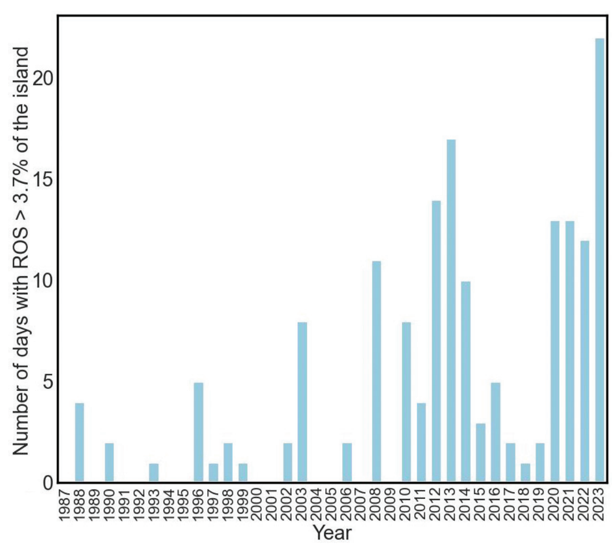

Fig. 3 Number of days with ROS covering more than 3.7% of the island during the fall (September–October) from 1987 to 2023, using the PMW detection algorithm (clustering with a GRP threshold at −2).

has been more frequent over the past 10 years (Table 2; ISHPCP 2022).

Large-scale ROS events

A total of 59 large-scale ROS events were detected during September and October between 1987 and 2023

Citation: *Polar Research* 2026, *45*, 12930, http://dx.doi.org/10.33265/polar.v45.12930

Table 4 Local accuracy metrics of PMW ROS detections at the three sites for the period September–October 1987–2023, when snow was on the ground.

Site	ROS detection method	TP	FN	TN	FP	Accuracy (%)	F1 score	Omission error (%)	Commission error (%)
Nangmagvik Lake	Clustering on GRP <-2	16	28	249	103	66.9	19.6	63.6	86.6
	GRP < −10	7	37	308	44	79.5	14.7	84.1	86.3
Sachs Harbour	Clustering on GRP < −2	12	67	722	313	65.9	5.9	84.8	96.3
	GRP < −10	7	72	846	189	76.6	5.1	91.1	96.4
Thomsen River	Clustering on GRP <-2	2	17	332	1	94.9	18.2	89.5	33.3
	GRP < −10	3	16	332	1	95.2	26.1	84.2	25.0
Sum of the three sites	Clustering on GRP < −2	30	112	1303	417	71.6	10.2	78.9	93.3
	GRP < −10	17	125	1486	234	80.7	8.7	88.0	93.2

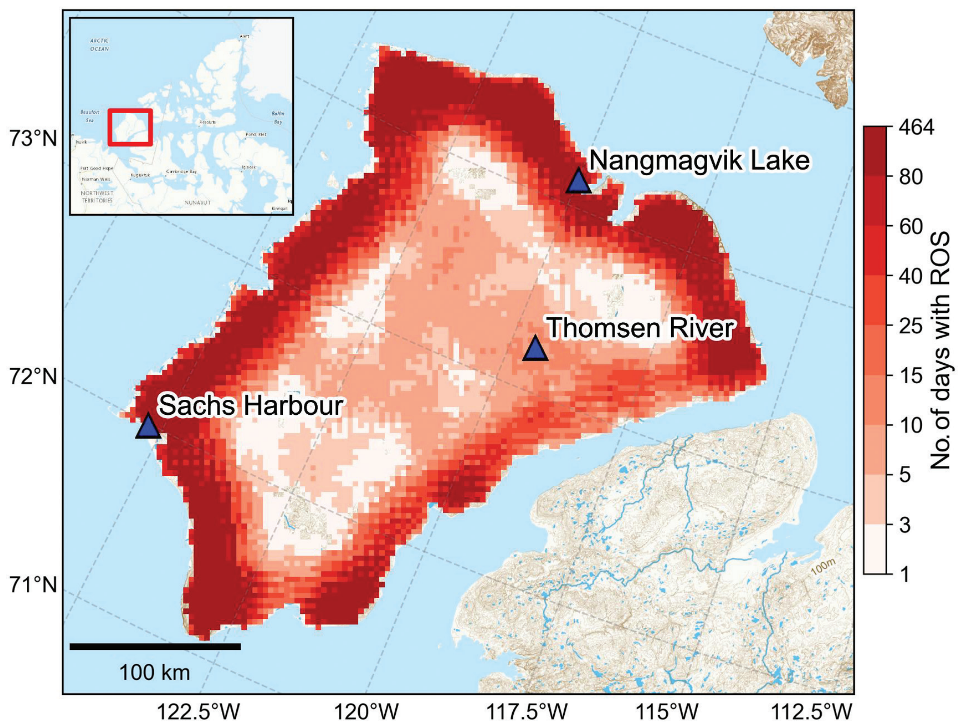

Fig. 4 Total number of days with ROS detected per pixel using PMW during September–October from 1987 to 2023.

(Table 5, Supplementary Table S3). Of these, 37 events were detected by at least one weather station and were therefore classified as TPs. Missing observations were frequent at the Thomsen River and Nangmagvik Lake stations and may have limited our ability to detect some ROS events using local weather data (Table 5). Most ROS events reported by community members (Table 3) were also detected using the PMW algorithm, with the exception of the event that occurred during the winter of 1987–88. Maps were created for each detected event to illustrate the spatial extent affected by ROS as identified using the PMW algorithm (Fig. 6, Supplementary Fig. S2).

We observe an increase in both the number and the duration of large-scale ROS events over time (Fig. 7).

We do not observe a significant increase in the intensity score of the large-scale ROS events over time (Fig. 8). However, the most intense ROS events detected by the PMW algorithm occurred more recently (post-2000).

Environmental and meteorological drivers of ROS

For 23 of the 59 large-scale ROS events detected between 1987 and 2023, an AR was present over Banks Island (39%). This proportion increases for large-scale ROS events that reached the interior of the island, compared to ROS events affecting only coastal areas. Eleven out of the 13 large-scale ROS events reaching the interior of the island were associated with the presence of an AR (85%). Results from the Mann-Whitney U test suggest that ARs are a potential driver of ROS intensity. All ROS intensity variables were significantly higher when an AR was present (Table 6).

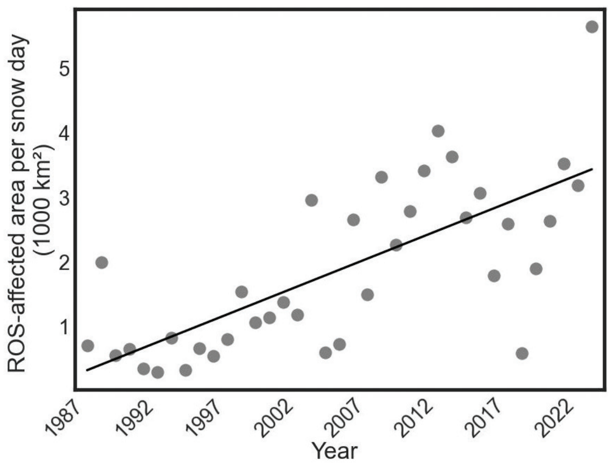

Fig. 5 Total area affected by ROS per day with snow during September–October for each year ($R^2 = 0.516$, $p < 0.001$).

The sea-ice anomaly was compared with two different ROS metrics; (a) the number of large-scale ROS events per year and (b) the total area affected by ROS, normalized by the number of snow days (September–October). The area affected by ROS is significantly higher when there is less sea ice around Banks Island (Fig. 9b, $R^2 = 0.678$, $p = 0.008$). The number of large-scale ROS events is also significantly higher ($R^2 = 0.336$, $p = 0.016$) when there is less sea ice around Banks Island in the fall (Fig. 9a); however, this relationship is weaker than that observed between sea-ice anomalies and the total area affected by ROS.

The only significant correlations between ROS metrics and climate oscillation patterns were for the PNA (Fig. 10). We observed a higher total area affected by ROS on Banks Island during positive phases of the PNA compared to negative phases, that is, lower index values (Spearman's $\rho = 0.446$, $p = 0.006$). No significant correlations were found between ROS metrics and the NAO and AO indices.

Discussion

As a result of our refinements in ROS detection, using both PMW algorithms and IQ, we were better able to

Table 5 ROS events detected using PMW with GRP < −2 with clustering (25 most intense ROS events).

Start date of event	Duration of events (days)	Total area affected by event (1000 km²)	Total precip. (mm)[a]	Intensity score	Events detected in Sachs Harbour	Events detected in Thomsen	Events detected in Nangmagvik
2008-10-03	10	47.7	30.1	1.00	False	Missing data	Missing data
2023-10-09	10	44.6	25.2	0.92	True	True	False
2022-10-04	9	16.6	17.4	0.59	True	True	True
1996-09-15	5	27.1	23.0	0.58	True	Missing data	True
2023-09-05	8	29.1	8.8	0.55	True	True	True
2012-10-03	10	18.3	9.4	0.55	True	Missing data	Missing data
2020-09-23	8	26.2	5.5	0.49	True	False	False
2013-09-24	9	22.2	4.1	0.49	True	Missing data	Missing data
1988-10-04	4	21.7	9.1	0.35	True	Missing data	Missing data
2003-10-02	4	27.4	2.5	0.32	True	Missing data	Missing data
2010-09-18	5	11.0	2.4	0.23	True	False	False
2021-09-26	4	12.7	3.9	0.23	True	True	Missing data
2014-09-08	5	11.8	0.7	0.22	True	Missing data	Missing data
2011-10-04	4	16.0	1.3	0.22	True	Missing data	Missing data
2015-09-29	2	22.5	1.0	0.19	True	Missing data	Missing data
2013-10-20	3	12.8	4.0	0.19	True	Missing data	Missing data
2003-10-09	3	7.6	6.1	0.18	False	Missing data	Missing data
2020-10-04	4	8.7	0.7	0.16	True	False	False
2006-10-12	2	7.6	6.9	0.15	True	False	Missing data
2010-09-27	3	7.2	3.6	0.15	False	False	False
2021-10-23	3	8.4	0.4	0.12	False	False	Missing data
1998-09-20	2	13.1	0.1	0.11	True	True	True
1990-09-21	2	6.9	4.4	0.11	True	Missing data	Missing data
2012-09-15	2	8.4	1.0	0.09	True	Missing data	False
2016-09-21	2	8.5	0.7	0.09	True	Missing data	Missing data

[a] ERA5.

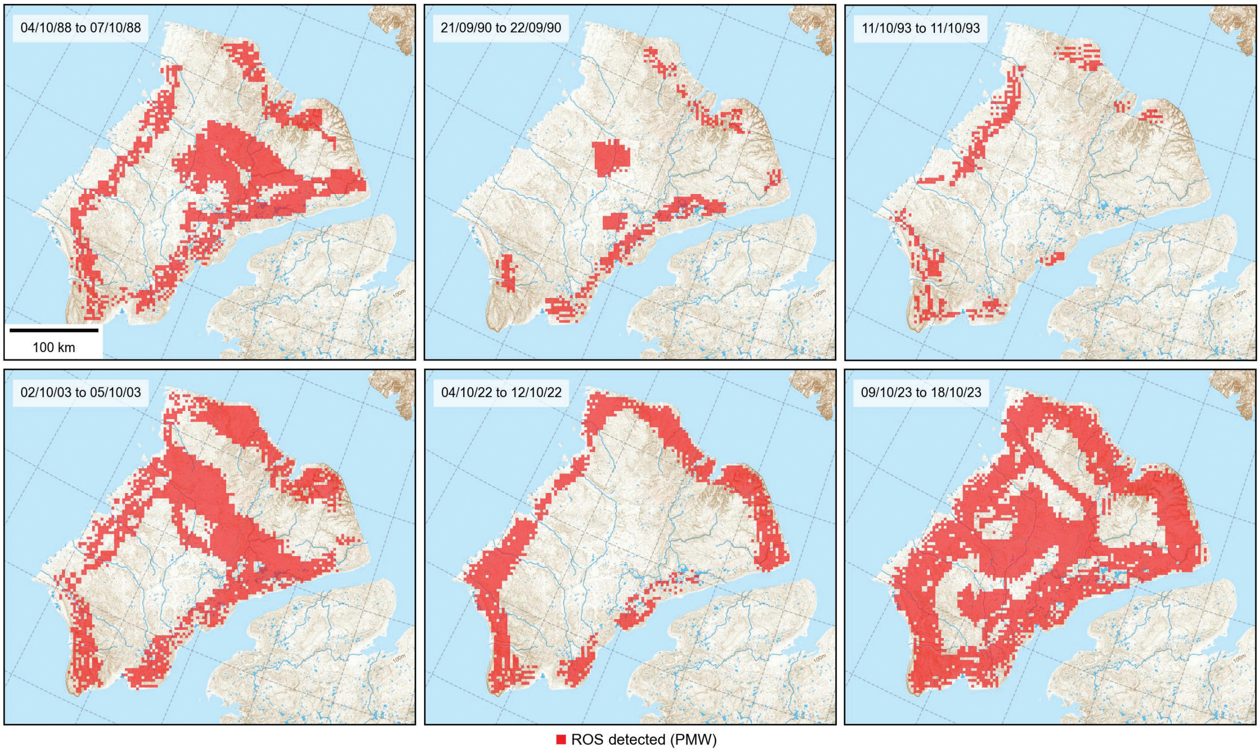

Fig. 6 Maps of large-scale ROS events detected using PMW imagery and also reported by community members.

characterize spatio-temporal trends in ROS. Our work allowed us to statistically confirm an increasing trend in ROS on Banks Island, consistent with previous findings for the CAA (Sasseville et al. 2024). These results are also consistent with IQ shared during interviews and workshops (ISHPCP 2022). We were also able to refine the spatial extent of ROS detection and identify a higher frequency of ROS in coastal areas of Banks Island.

Our ability to assess TPs in the detection of large-scale ROS events was hampered by gaps in data from weather stations; however, IQ related to ROS helped address some of these gaps. The use of a higher threshold (-2) combined with a clustering algorithm resulted in an increase in F1-scores based on local validation at two out of three weather stations. This modified algorithm increased the number of TP ROS events overall, but it also resulted in an increased in false positives. Despite generally low F1-scores based on the local validation, the algorithm for detecting large-scale ROS events across the island still shows promise. Sixty-four percent of the large-scale ROS events were confirmed by IQ and/or by at least one of the three weather stations. However, it remains unclear whether existing documentation of past ROS events from IQ is comprehensive. More targeted workshops and interviews that focused specifically on compiling inventories of past ROS events in the CAA would help address this limitation in future work.

This work allowed for the identification of specific dates of large-scale ROS events and the characterization of their intensity. This represents an important advance in linking the characteristics of large-scale ROS events to their potential consequences for large herbivore populations. We believe this work can inform recovery strategies for caribou and help local communities to better understand how ROS events affect this culturally important species and how climate change might increase their occurrence and intensity over time. However, the effects of recent ROS events on herbivore die-offs and caribou population trends remain unclear. Despite the observed increase in the frequency of large-scale ROS events on Banks Island, we also observed a recent increase in the population size of Peary caribou on the island (Davison et al. 2017; SARC 2022). Most ROS events reported by communities as having impacted Peary caribou occurred before 2003. Although an increase in the frequency of ROS has been observed by Ikaahuk community members (Riedlinger 2001; ISHPCP 2022), it was also reported by many Arctic communities that icing events have been less frequent after 2010 than before (SARC 2022). It is possible that environmental conditions during more recent ROS events were not amenable to formation of ice layers within the snowpack. Depending on precipitation amount, snow depth and temperature, a ROS event may expose pasture rather than lead to ice formation (Loe et al. 2021).

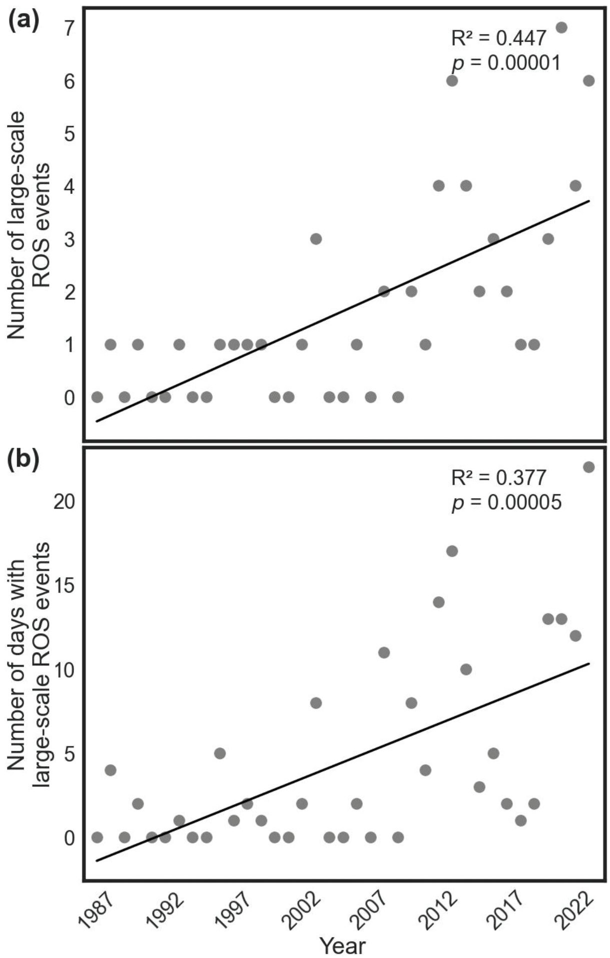

Fig. 7 (a) Number of large-scale ROS events and (b) total duration of large-scale ROS events on Banks Island in the fall (September–October).

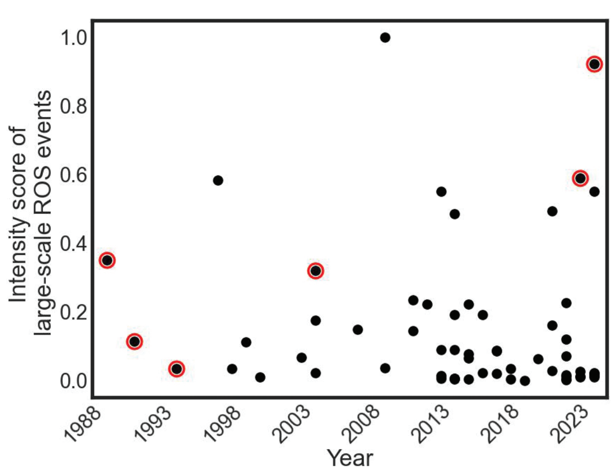

Fig. 8 Intensity score of large-scale ROS events. Red circles indicate ROS events that were both detected by the PMW algorithm and reported by community members.

Further work is needed to validate this hypothesis through future workshops and interviews, as well as through analyses of weather conditions before and after ROS events. Recent research also questions the net effects of icing events on herbivore populations. Loe et al. (2021) showed that warmer autumn can buffer the impacts of severe icy winters, and Hansen et al. (2019) demonstrated that the impacts of ROS on Svalbard reindeer populations are density-dependent. These findings suggests that populations may be more resilient and less sensitive to extreme events when population densities are low (Hansen et al. 2019). Riedlinger (2001) reported an interview with an Ikaahuk resident regarding the impacts of the increased rainfall and longer summers on herbivores who stated: "It is hard to see that—because when changes start occurring here, well … the caribou population is down, and so how can you really tell?" (Riedlinger 2001). This observation may also suggest a density-dependent effect, potentially explaining the limited impacts of recent ROS events on Peary caribou populations that currently occur at low densities on Banks Island. In contrast, muskox populations on Banks Island were high according to recent surveys but are currently experiencing a decline (Davison et al. 2017; SARC 2022). This density-dependent effect of ROS could potentially help explain the observed decline in muskox populations, as they may have been more vulnerable to recent ROS events because of higher population densities. Differences in space use between caribou and muskoxen may also contribute to their differential vulnerability to ROS events (Forchhammer et al. 2002). For example, the 2003 ROS event that resulted in muskox mortality occurred in northern Banks Island, whereas caribou typically spend the winter in the southern part of the island (Grenfell & Putkonen 2008). Clearly, more research is needed to better understand the impacts of ROS events on ungulate populations (Davison et al. 2017).

A substantial proportion of the large-scale ROS events detected on Banks Island (39%) were associated with ARs, and this proportion increased to 85% when considering only the large-scale ROS events that reached the interior of the island. ROS intensity was also significantly higher when ARs occurred over Banks during a ROS event (Table 6). This observation is consistent with past research showing linkages between large-scale ROS events in the Arctic and ARs (Bokhorst et al. 2016; Wickström et al. 2020; Voveris & Serreze 2023). There was also a relationship between sea-ice concentration and both the number of ROS events and the total area affected by ROS in the fall, with the effect being more pronounced for the latter. Our results are similar to previous studies showing the influence of sea-ice concentration on local precipitation (Bintanja & Selten 2014;

Citation: *Polar Research* 2026, *45*, 12930, http://dx.doi.org/10.33265/polar.v45.12930

Table 6 Mann-Whitney U test of ROS intensity variables grouped by the presence of atmospheric rivers during events.

ROS intensity variables	Mann-Whitney *U*	*p*
Total area affected by event	153	< 0.001
Duration of event	174	< 0.001
Total precipitation (ERA5)	165	< 0.001
ROS intensity score	141	< 0.001

Forbes et al. 2016; Wickström et al. 2020). Therefore, both local drivers, such as open water, and remote sources affecting atmospheric conditions over Banks Island appear to play a role in the occurrence and intensity of ROS events on Banks.

We found a statistically significant correlation with PNA climate oscillation patterns, but not with NAO or AO. These results are consistent with previous studies demonstrating the relationship between the positive phase of the PNA and reductions in sea-ice extent in the western Arctic through increases in air temperature (L'Heureux et al. 2008; Liu et al. 2021).

Our work focused on Banks Island. The method could be applied to other islands of the CAA, where die-off and icing events have been reported by local communities, to examine regional variation in the spatial patterns and consequences of ROS for wildlife (Taylor 2005; Johnson et al. 2016; AGFPCP 2024). The influence of Pacific and Atlantic air masses creates major differences in precipitation and temperature, and variation in topography also plays a role in local weather conditions (COSEPAC 2015). In Aujuittuq, the northernmost community in Canada, people reported that ROS events were more likely to affect muskoxen occupying lowland valleys than caribou in hilly areas because rain would transition to snow with increasing elevation (AGFPCP 2024). It would be interesting to extend the application of the approach proposed in this paper to other islands of the CAA. We expect to find differences in spatio-temporal patterns as well as in correlations with environmental and meteorological drivers.

Community members mentioned that rain falling just before the arrival of snow is also critical and can lead to ice-locked pasture (ICBPCP 2023). Similarly, shallow snow depth or melting snow may facilitate the formation of ground-fast ice crusts. Our algorithm only detects the presence of water on the surface of the snowpack (Dolant et al. 2016). However, not all ROS events lead to the creation of an ice crust, and other events can also result in ice formation, notably periods of snowmelt followed by cooling, and rain occurring just before the freezing period. The use of C-Band radar could potentially help with the detection of melting snow (Vickers et al. 2022). Bartsch et al. (2023) propose

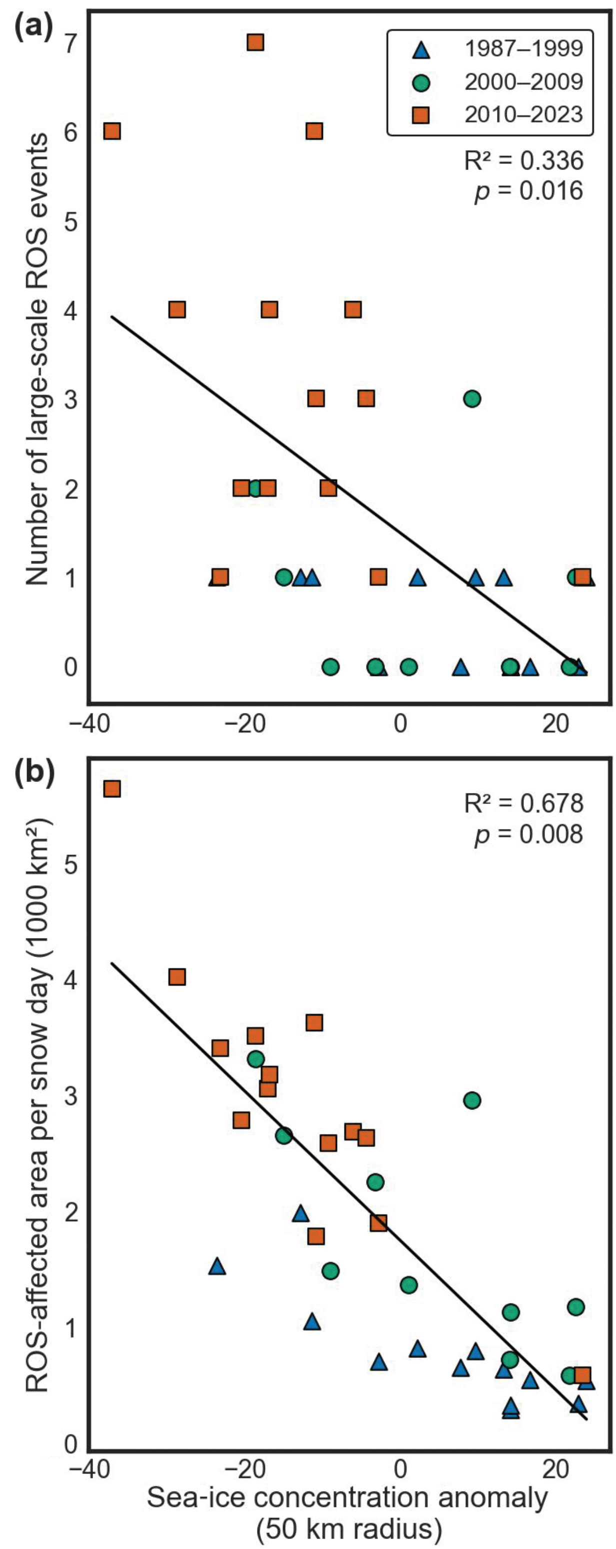

Fig. 9 (a) Number of large-scale ROS events and (b) total area affected by ROS (1000 km^2) in relation to fall sea-ice concentration anomalies on Banks Island.

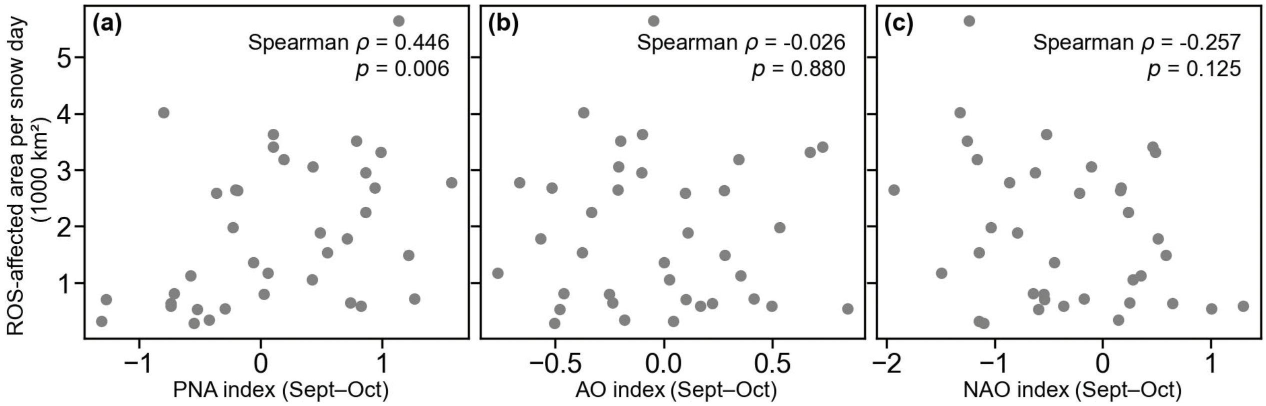

Fig. 10 Total area affected by ROS (1000 km²) on Banks Island in relation to (a) PNA index, (b) AO index and (c) NAO index.

using a fusion of passive and active sensors to develop long-term ROS monitoring capacity in the Arctic. The combination of these data sets could also be useful for detecting ice layers in the snowpack, which would be of interest for characterizing potential consequences for herbivores (Montpetit et al. 2013; Langlois et al. 2017; Bartsch et al. 2023). The ability to map the spatial patterns of ice layers in the snowpack would increase our capacity to determine whether an icing event could lead to population die-off, reduced reproduction rates or changes in animal movement. It would also make it possible to better understand the environmental and meteorological factors that lead to the creation of ice layers in the snowpack following a melt or ROS event.

Conclusion

Our work highlights the value of PMW and IQ in identifying large-scale ROS events in the CAA. The GRP algorithm proposed by Dolant et al. (2016) can be leveraged to study ROS events in the CAA, where the lack of weather station data and the remoteness make such analyses challenging. Our study also highlights how IQ of the land, sea and wildlife is key to understanding ROS events. IQ describe the timing of ROS events, their spatial distribution, the conditions driving them and their consequences for wildlife (ISHPCP 2022, 2023; ICBPCP 2023). As climate change continues to transform the Arctic environment, weaving scientific approaches with IQ will be essential to understand the impacts on wildlife and people and to support meaningful adaptation measures.

Acknowledgements

The authors are extremely grateful to the Inuvialuit and Inuit communities who shared their knowledge of ROS and Peary caribou. Specifically, the authors thank the following knowledge-holders for their participation in this project: Joey Carpenter, John Lucas Jr., Wayne Gully, Warren Esay, George Aklah, Joe Ashevak, Aleeasuk Idiout and Jarloo Kiguktuk. The authors also thank the following organizations: the Sachs Harbour Hunters & Trappers Committee; the Taloyoak Umaruliririgut Association; the Iviq Hunters & Trappers Association; and the Resolute Bay Hunters & Trappers Association. ChatGPT (https://chat.openai.com/) was used to assist with the development of Python code for data processing in this study. They also acknowledge the use of DeepL (https://www.deepl.com/en/translator) to translate parts of the introduction and methodology sections from French (first author's mother tongue) to English. All content was originally created, reviewed and edited by the authors.

Disclosure statement

The authors report no conflict of interest.

Funding

This project was funded by the Natural Sciences and Engineering Research Council of Canada, the Fonds de Recherche du Québec—Nature et Technologies, Environment and Climate Change Canada, Polar Knowledge Canada, and the Center for Northern Studies.

References

Akosa J.S. 2017. Predictive accuracy: a misleading performance measure for highly imbalanced data. Paper 942-2017. Proceedings SAS Global Forum 2017 Conference. Cary, NC: SAS Institute Inc. Accessed on the internet at https://support.sas.com/resources/papers/proceedings17/ on 25 March 2025.

Arctic Council Indigenous Peoples' Secretariat 2018. *Ottawa Indigenous Knowledge principles*. Ottawa: Arctic Council. Accessed on the internet at https://www.arcticpeoples.com/knowledge#indigenous-knowledge on 22 July 2026.

AGFPCP (Aujuittuq [Grise Fiord] PCP interviews) 2024. Workshop on Peary caribou habitat and snow conditions using participatory mapping, fuzzy cognitive mapping, and individual semi-directed interviews with the community of Aujuittuq (Grise Fiord), NU. Facilitated by Cheryl Johnson, Estéban Hamel Jomphe, & Josée-Anne Langlois; in partnership with the Iviq Hunters & Trappers Association and The Peary Caribou Project, March.

AGFPCP (Aujuittuq [Grise Fiord] PCP interviews) 2025. Workshop on snow conditions and Peary caribou using fuzzy cognitive mapping, and semi-directed interviews and validation of work on rain-on-snow and disturbances with the community of Aujuittuq (Grise Fiord), NU. Facilitated by Cheryl Johnson & Josée-Anne Langlois; in partnership with the Iviq Hunters & Trappers Association and The Peary Caribou Project, November and December.

Bartsch A., Bergstedt H., Pointner G., Muri X., Rautiainen K., Leppänen L., Joly K., Sokolov A., Orekhov P., Ehrich D. & Soininen E.M. 2023. Towards long-term records of rain-on-snow events across the Arctic from satellite data. *The Cryosphere 17*, 889–915, doi: 10.5194/tc-17-889-2023.

Bartsch A., Kumpula T., Forbes B.C. & Stammler F. 2010. Detection of snow surface thawing and refreezing in the Eurasian Arctic with QuikSCAT: implications for reindeer herding. *Ecological Applications 20*, 2346–2358, doi: 10.1890/09-1927.1.

Bergman C.M., Schaefer J.A. & Luttich S.N. 2000. Caribou movement as a correlated random walk. *Oecologia 123*, 364–374, doi: 10.1007/s004420051023.

Bintanja R. 2018. The impact of Arctic warming on increased rainfall. *Scientific Reports 8*, article no. 16001, doi: 10.1038/s41598-018-34450-3.

Bintanja R. & Selten F.M. 2014. Future increases in Arctic precipitation linked to local evaporation and sea-ice retreat. *Nature 509*, 479–482, doi: 10.1038/nature13259.

Bokhorst S., Pedersen S.H., Brucker L., Anisimov O., Bjerke J.W., Brown R.D., Ehrich D., Essery R.L.H., Heilig A., Ingvander S., Johansson C., Johansson M., Jónsdóttir I.S., Inga N., Luojus K., Macelloni G., Mariash H., McLennan D., Rosqvist G.N., Sato A., Savela H., Schneebeli M., Sokolov A., Sokratov S.A., Terzago S., Vikhamar-Schuler D., Williamson S., Qiu Y. & Callaghan T.V. 2016. Changing Arctic snow cover: a review of recent developments and assessment of future needs for observations, modelling, and impacts. *Ambio 45*, 516–537, doi: 10.1007/s13280-016-0770-0.

Brodzik M.J. & Long D.G. 2018. *Calibrated Passive Microwave Daily EASE-Grid 2.0 Brightness Temperature ESDR (CETB). Algorithm theoretical basis document. Revision 1.0*. National Snow and Ice Data Center.

Brodzik M.J., Long D.G., Hardman M.A., Paget A. & Armstrong R. 2016. MEaSUREs Calibrated Enhanced-Resolution Passive Microwave Daily EASE-Grid 2.0 Brightness Temperature ESDR, Version 1. Boulder, National Snow and Ice Data Center Distributed Active Archive Center, doi: 10.5067/MEASURES/CRYOSPHERE/NSIDC-0630.001

COSEPAC 2015. *Évaluation et rapport de situation du COSEPAC sur le caribou de Peary, Rangifer tarandus pearyi, au Canada. (COSEWIC assessment and status report on the Peary caribou, Rangifer tarandus pearyi, in Canada.)* Ottawa: Committee on the Status of Endangered Wildlife in Canada.

Davison T., Williams J. & Adamczewski J. 2017. *Aerial survey of Peary caribou (Rangifer tarandus pearyi) and muskoxen (Ovibos moschatus) on Banks Island, July 2014. Manuscript Report 270*. Yellowknife, NT: Environment and Natural Resources, Government of Northwest Territories.

Dolant C., Langlois A., Brucker L., Royer A., Roy A. & Montpetit B. 2017. Meteorological inventory of rain-on-snow events in the Canadian Arctic Archipelago and satellite detection assessment using passive microwave data. *Physical Geography 39*, 428–444, doi: 10.1080/02723646.2017.1400339.

Dolant C., Langlois A., Montpetit B., Brucker L., Roy A. & Royer A. 2016. Development of a rain-on-snow detection algorithm using passive microwave radiometry. *Hydrological Processes 30*, 3184–3196, doi: 10.1002/hyp.10828.

Eira I.M.G., Jaedicke C., Magga O.H., Maynard N.G., Vikhamar-Schuler D. & Mathiesen S.D. 2013. Traditional Sámi snow terminology and physical snow classification—two ways of knowing. *Cold Regions Science and Technology 85*, 117–130, doi: 10.1016/j.coldregions.2012.09.004.

Environment and Climate Change Canada 2022. *Recovery strategy for the Peary caribou (Rangifer tarandus pearyi) in Canada*. Ottawa: Environment and Climate Change Canada.

Ester M., Kriegel H.-P., Sander J. & Xu X. 1996. A density-based algorithm for discovering clusters in large spatial databases with noise. In E. Simoudis et al. (eds.): *KDD'96: proceedings of the Second International Conference on Knowledge Discovery and Data Mining*. Pp. 226–231. Portland, OR: AAAI Press.

Forbes B.C., Kumpula T., Meschtyb N., Laptander R., Macias-Fauria M., Zetterberg P., Verdonen M., Skarin A., Kim K.-Y., Boisvert L.N., Stroeve J.C. & Bartsch A. 2016. Sea ice, rain-on-snow and tundra reindeer nomadism in Arctic Russia. *Biology Letters 12*, article no. 20160466, doi: 10.1098/rsbl.2016.0466.

Forchhammer M.C., Post E., Stenseth N.C. & Boertmann D.M. 2002. Long-term responses in Arctic ungulate dynamics to changes in climatic and trophic processes. *Population Ecology 44*, 113–120, doi: 10.1007/s101440200013.

Government of Canada 2021. Canadian Ice Service Weekly regional ice charts. Accessed on the internet at https://iceweb1.cis.ec.gc.ca/Archive/page1.xhtml?lang=en on 16 December 2022.

Grenfell T.C. & Putkonen J. 2008. A method for the detection of the severe rain-on-snow event on Banks Island, October 2003, using passive microwave remote sensing. *Water Resources Research 44*, W03425, doi: 10.1029/2007WR005929.

Gunn A., Miller F.L., Barry S.J. & Buchan A. 2006. A near-total decline in caribou on Prince of Wales, Somerset, and Russell islands, Canadian Arctic. *Arctic 59*, 23–36, doi: 10.14430/arctic358.

Hansen B.B., Gamelon M., Albon S.D., Lee A.M., Stien A., Irvine R.J., Sæther B.-E., Loe L.E., Ropstad E., Veiberg V. & Grøtan V. 2019. More frequent extreme climate events stabilize reindeer population dynamics. *Nature Communications 10*, article no. 1616, doi: 10.1038/s41467-019-09332-5.

Hansen B.B., Isaksen K., Benestad R.E., Kohler J., Pedersen Å.Ø., Loe L.E., Coulson S.J., Larsen J.O. & Varpe Ø. 2014. Warmer and wetter winters: characteristics and implications of an extreme weather event in the High Arctic. *Environmental Research Letters 9*, article no. 114021, doi: 10.1088/1748-9326/9/11/114021.

ISHPCP (Ikaahuk [Sachs Harbour] PCP workshop) 2022. Workshop on Peary caribou and observed environmental changes using participatory mapping and individual semi-directed interviews with the community of Ikaahuk (Sachs Harbour), NWT. Facilitated by Cheryl Johnson, Isabelle Duclos, Jillian Wettlaufer Susie & Memeogana; in partnership with the Sachs Harbour Hunters & Trappers Committee and The Peary Caribou Project, October.

ISHPCP (Ikaahuk [Sachs Harbour] PCP workshop) 2023. Workshop on muskox and Peary caribou using participatory mapping, proportional piling, fuzzy cognitive mapping, and semi-directed interviews with the community of Ikaahuk (Sachs Harbour), NWT. Facilitated by Léna Bureau, Cheryl Johnson, Susie Memogana & Alex Pantis; in partnership with the Sachs Harbour Hunters & Trappers Committee and The Peary Caribou Project, October.

ISHPCP (Ikaahuk [Sachs Harbour] PCP workshop) 2025. Workshop on snow conditions and Peary caribou using fuzzy cognitive mapping, and semi-directed interviews and validation of work on rain-on-snow and disturbances with the community of Ikaahuk (Sachs Harbour), NWT. Facilitated by Cheryl Johnson, & Josée-Anne Langlois; in partnership with the Sachs Harbour Hunters & Trappers Committee, and The Peary Caribou Project, September.

ICBPCP (Iqaluktuuttiaq [Cambridge Bay] PCP workshop) 2023. Workshop on observed environmental changes and rain-on-snow conditions using participatory mapping and semi-directed interviews with the communities of Iqaluktuuttiaq (Cambridge Bay), NU, Ikaahuk (Sachs Harbour), NWT, Taloyoak, NU, Tuktoyaktuk, NWT, and Ulukhaktok, NWT. Facilitated by Josée-Anne Langlois, Léna Bureau & Cheryl Johnson; in partnership with the Ekaluktutiak Hunters & Trappers Association, Sachs Harbour Hunters & Trappers Committee, Tuktokaytuk Hunters & Trappers Committee, Olokhaktomiut Hunters & Trappers Committee, Taloyoak Umaruliririgut Association and The Peary Caribou Project, April.

Johnson C.A., Neave E., Blukacz-Richards E.A., Banks S.N. & Quesnelle P.E. 2016. *Knowledge assessment (community and scientific) to inform the identification of critical habitat for Peary caribou, Rangifer tarandus pearyi, in the Canadian Arctic.* Ottawa: Environment and Climate Change Canada, Science and Technology.

Jolly D., Berkes F., Castleden J. & Nichols T. 2002. We can't predict the weather like we used to: Inuvialuit observations of climate change, Sachs Harbour, western Canadian Arctic. In I. Krupnik & D. Jolly (eds.): *The Earth is faster now: indigenous observations of Arctic environmental change*. Pp. 92–125. Fairbanks, AK: Arctic Research Consortium of the United States.

Kaluskar S., Johnson C.A., Blukacz-Richards E.A., Ouellet F., Kim D.-K. & Arhonditsis G. 2020. A stochastic modelling framework to accommodate the inter-annual variability of habitat conditions for Peary caribou (*Rangifer tarandus pearyi*) populations. *Ecological Informatics 56*, article no. 101013, doi: 10.1016/j.ecoinf.2019.101013.

Laidler G.J., Elee P., Ikummaq T., Joamie E. & Aporta C. 2010. Mapping Inuit sea ice knowledge, use, and change in Nunavut, Canada (Cape Dorset, Igloolik, Pangnirtung). In I. Krupnik et al. (eds): *SIKU: knowing our ice: documenting Inuit sea ice knowledge and use*. Pp. 45–80. Dordrecht: Springer.

Laidler G.J. & Grimwood B. 2010. *Report on the results of a research planning workshop in: Gjoa Haven*. Accessed on the internet at https://straightupnorth.files.wordpress.com/2020/05/gh_2010_02_workshopreport_en.pdf on 16 December 2022.

Langlois A., Johnson C.A., Montpetit B., Royer A., Blukacz-Richards E.A., Neave E., Dolant C., Roy A., Arhonditsis G., Kim D.K., Kaluskar S. & Brucker L. 2017. Detection of rain-on-snow (ROS) events and ice layer formation using passive microwave radiometry: a context for Peary caribou habitat in the Canadian Arctic. *Remote Sensing of Environment 189*, 84–95, doi: 10.1016/j.rse.2016.11.006.

Laptander R. 2023. The Yamal Nenets' traditional and contemporary environmental knowledge of snow, ice, and permafrost. *Ecology and Society 28*, article no. 6, doi: 10.5751/ES-14353-280306.

Larter N.C. & Nagy J.A. 1994. *Ice conditions survey, Banks Island October/November 1993. Manuscript Report 77*. Inuvik, NWT: Department of Renewable Resources, Government of the Northwest Territories.

Leclerc L.-M. & Boulanger J. 2018. *Population estimate of the Dolphin and Union caribou herd (Rangifer tarandus groenlandicus x pearyi). Coastal survey, October 2018 and demographic indicators*. Kugluktuk, NU: Nunavut Department of Environment, Wildlife Research Section.

L'Heureux M.L., Kumar A., Bell G.D., Halpert M.S. & Higgins R.W. 2008. Role of the Pacific-North American (PNA) pattern in the 2007 Arctic sea ice decline. *Geophysical Research Letters 35*, L20701, doi: 10.1029/2008GL035205.

Liebe H.J. 1989. MPM—an atmospheric millimeter-wave propagation model. *International Journal of Infrared and Millimeter Waves 10*, 631–650, doi: 10.1007/BF01009565.

Liu Z., Risi C., Codron F., He X., Poulsen C., Wei Z., Chen D., Li S. & Bowen G. 2021. Acceleration of western Arctic sea ice loss linked to the Pacific North American pattern. *Nature Communications 12*, article no. 1519, doi: 10.1038/s41467-021-21830-z.

Ljubicic G.J., Mearns R., Okpakok S. & Robertson S. 2022. Nunami iliharniq (learning from the land): reflecting on relational accountability in land-based learning and cross-cultural research in Uqšuqtuuq (Gjoa Haven, Nunavut). *Arctic Science 8*, 252–291, doi: 10.1139/as-2020-0059.

Ljubicic G.J., Robertson S., Mearns R. & Okpakok S. 2016. Connecting Inuit elders and youth: learning about caribou, community, and well-being in Gjoa Haven, Nunavut (2011–2016). Accessed on the internet at https://straightupnorth.ca/caribou-and-community-well-being/ on 16 December 2022.

Loe L.E., Liston G.E., Pigeon G., Barker K., Horvitz N., Stien A., Forchhammer M., Getz W.M., Irvine R.J., Lee A., Movik L.K., Mysterud A., Pedersen Å.Ø., Reinking A.K., Ropstad E., Trondrud L.M., Tveraa T., Veiberg V., Hansen B.B. & Albon S.D. 2021. The neglected season: warmer autumns counteract harsher winters and promote population growth in Arctic reindeer. *Global Change Biology 27*, 993–1002, doi: 10.1111/gcb.15458.

Mallory C.D. & Boyce M.S. 2018. Observed and predicted effects of climate change on Arctic caribou and reindeer. *Environmental Reviews 26*, 13–25, doi: 10.1139/er-2017-0032.

Markkula I., Turunen M. & Rasmus S. 2019. A review of climate change impacts on the ecosystem services in the Saami Homeland in Finland. *Science of the Total Environment 692*, 1070–1085, doi: 10.1016/j.scitotenv.2019.07.272.

Maxwell J.B. 1981. Climatic regions of the Canadian Arctic Islands. *Arctic 34*, 225–240, doi: 10.14430/arctic2525.

Meier W.N., Petty A., Hendricks S., Perovich D., Farrell S., Webster M., Divine D., Kaleschke L., Ricker R. & Tian-Kunze X. 2022. *Arctic Report Card 2022: sea ice. NOAA Technical Report OAR ARC 22.06*. Accessed on the internet at 10.25923/xyp2-vz45 on 24 January 2023.

Mesinger F., DiMego G., Kalnay E., Mitchell K., Shafran P.C., Ebisuzaki W., Jović D., Woollen J., Rogers E., Berbery E.H., Ek M.B., Fan Y., Grumbine R., Higgins W., Li H., Lin Y., Manikin G., Parrish D. & Shi W. 2006. North American Regional Reanalysis. *Bulletin of the American Meteorological Society 87*, 343–360, doi: 10.1175/BAMS-87-3-343.

Miller F.L. & Gunn A. 2003. Status, population fluctuations and ecological relationships of Peary caribou on the Queen Elizabeth Islands: implications for their survival. *Rangifer 23*, *Spec. Iss. 14,* 213–226, doi: 10.7557/2.23.5.1703.

Mo R. 2024. EDARA: an ERA5-based dataset for atmospheric river analysis. *Scientific Data 11*, article no. 900, doi: 10.1038/s41597-024-03679-1.

Montpetit B., Royer A., Roy A., Langlois A. & Derksen C. 2013. Snow microwave emission modeling of ice lenses within a snowpack using the microwave emission model for layered snowpacks. *IEEE Transactions on Geoscience and Remote Sensing 51*, 4705–4717, doi: 10.1109/TGRS.2013.2250509.

Mooney P.A. & Li L. 2021. Near future changes to rain-on-snow events in Norway. *Environmental Research Letters 16*, article no. 064039, doi: 10.1088/1748-9326/abfdeb.

Nagy J.A. & Gunn A. 2004. *Productivity of Peary caribou and Muskoxen on Banks Island and Melville islands, NT, July 2004. Manuscript Report 2004.* Yellowknife: Department of Environment and Natural Resources. Government of Northwest Territories.

Nagy J.A., Larter N. & Wright W.H. 2013. *Population estimates for Peary caribou and muskox on Banks Island, NWT, July 1994. Manuscript Report 223.* Yellowknife: Department of Environment and Natural Resources. Government of Northwest Territories.

Nagy J.A., Larter N.C. & Fraser V.P. 1996. Population demography of Peary caribou and muskox on Banks Island, N.W.T., 1982–1992. *Rangifer 16, Spec. Iss. 9,* doi: 10.7557/2.16.4.1245.

Nancarrow T.L. & Chan H.M. 2010. Observations of environmental changes and potential dietary impacts in two communities in Nunavut, Canada. *Rural and Remote Health 10*, article no. 1370, doi: 10.22605/RRH1370.

Natural Resources Canada 2014. Atlas of Canada National Scale Data 1:1,000,000. Boundary Polygons. Open Government Portal. Data set. Accessed on the internet at https://open.canada.ca/data/en/dataset/fec926ca-25ad-5c92-a9a7-6009c21d17b3 on 16 October 2024.

Natural Resources Canada 2016a. Canada Base Map Transportation (CBMT) – CBMT – Canada Base Map – Transportation (tiled version) (EPSG:3978) (English) – Open Government Portal. Data set. Accessed on the internet at https://open.canada.ca/data/en/dataset/296de17c-001c-4435-8f9a-f5acab632e85 on 16 October 2024.

Natural Resources Canada 2016b. National Parks and National Park Reserves of Canada Legislative Boundaries. Open Government Portal. Data set. Accessed on the internet at https://open.canada.ca/data/en/dataset/9e1507cd-f25c-4c64-995b-6563bf9d65bd on 16 October 2024.

Natural Resources Canada 2024. High Resolution Digital Elevation Model Mosaic (HRDEM Mosaic). CanElevation Series. Open Government Portal. Data set. Accessed on the internet at https://open.canada.ca/data/en/dataset/0fe65119-e96e-4a57-8bfe-9d9245fba06b on 16 October 2024.

NWT Bureau of Statistics 2024. NWT Bureau of Statistics. Sachs Harbour. NWT Bureau of Statistics. Accessed on the internet at https://www.statsnwt.ca/community-data/infrastructure/Sachs_harbour.html on 25 March 2025.

Paquette E., Ljubicic G., Johnson C.A., Okpakok S., Mueller D. & Montpetit B. 2023. Seasonal sea ice conditions affect caribou crossing areas around Qikiqtaq, Nunavut: Uqsuqtuurmiut knowledge guides ice chart analysis. *Arctic 76*, 83–101, doi: 10.14430/arctic77149.

Pearce T.D., Ford J.D., Laidler G.J., Smit B., Duerden F., Allarut M., Andrachuk M., Baryluk S., Dialla A., Elee P., Goose A., Ikummaq T., Joamie E., Kataoyak F., Loring E., Meakin S., Nickels S., Shappa K., Shirley J. & Wandel J. 2009. Community collaboration and climate change research in the Canadian Arctic. *Polar Research 28*, 10–27, doi: 10.1111/j.1751-8369.2008.00094.x.

Pulliainen J.T., Grandell J. & Hallikainen M.T. 1999. HUT snow emission model and its applicability to snow water equivalent retrieval. *IEEE Transactions on Geoscience and Remote Sensing 37*, 1378–1390, doi: 10.1109/36.763302.

Putkonen J. & Roe G. 2003. Rain-on-snow events impact soil temperatures and affect ungulate survival. *Geophysical Research Letters 30*, article no. 1188, doi: 10.1029/2002GL016326.

QRBPCP (Qausuittuq [Resolute Bay] PCP interviews) 2024. Workshop on Peary caribou habitat and snow conditions using participatory mapping, fuzzy cognitive mapping, and semi-directed interviews with the community of Qausuittuq (Resolute Bay), NU. Facilitated by Cheryl, Johnson, Estéban Hamel Jomphe, Josée-Anne Langlois& Alexandre Roy; in partnership with the Resolute Bay Hunters & Trappers Association and The Peary Caribou Project, January.

QRBPCP (Qausuittuq [Resolute Bay] PCP interviews) 2025. Workshop on snow conditions and Peary caribou using fuzzy cognitive mapping, and semi-directed interviews and validation of work on rain-on-snow and disturbances with the community of Qausuittuq (Resolute Bay), NU. Facilitated by Cheryl Johnson, Josée-Anne Langlois, & Alexandre Roy; in partnership with the Resolute Bay Hunters & Trappers Association and The Peary Caribou Project, November.

Ramsay B.H. 1998. The interactive multisensor snow and ice mapping system. *Hydrological Processes 12*, 1537–1546, doi: 10.1002/(SICI)1099-1085(199808/09)12:10/11<1537::AID-HYP679>3.0.CO;2-A.

Rantanen M., Karpechko A.Y., Lipponen A., Nordling K., Hyvärinen O., Ruosteenoja K., Vihma T. & Laaksonen A. 2022. The Arctic has warmed nearly four times faster than the globe since 1979. *Communications Earth & Environment 3*, article no. 168, doi: 10.1038/s43247-022-00498-3.

Rennert K.J., Roe G., Putkonen J. & Bitz C.M. 2009. Soil thermal and ecological impacts of rain on snow events in the circumpolar Arctic. *Journal of Climate 22*, 2302–2315, doi: 10.1175/2008JCLI2117.1.

Riedlinger D. 2001. *Community-based assessments of change, contributions of Inuvialuit knowledge to understanding climate change in the Canadian Arctic*. Master's thesis, University of Manitoba.

Robinson D.A. & Estilow T.W. 2021. Rutgers Northern Hemisphere 24 km Weekly Snow Cover Extent, September 1980 Onward. Version 1. Accessed on the internet at https://nsidc.org/data/g10035/versions/1 on 13 November 2024.

Robinson D.A., Estilow T.W. & NOAA CDR Program 2012. NOAA Climate Data Record (CDR) of Northern Hemisphere (NH) Snow Cover Extent (SCE). Accessed on the internet at https://www.ncei.noaa.gov/access/metadata/landing-page/bin/iso?id=gov.noaa.ncdc:C00756 on 2 July 2024.

Roy A., Royer A., Wigneron J.-P., Langlois A., Bergeron J. & Cliche P. 2012. A simple parameterization for a boreal forest radiative transfer model at microwave frequencies. *Remote Sensing of Environment 124*, 371–383, doi: 10.1016/j.rse.2012.05.020.

SARC 2012. *Species status report for Peary caribou (Rangifer tarandus pearyi) in the Northwest Territories*. Yellowknife, NT: Species at Risk Committee.

SARC 2022. *Species status report for Peary caribou (Rangifer tarandus pearyi) in the Northwest Territories*. Yellowknife, NT: Species at Risk Committee.

Sasseville V., Langlois A., Brucker L. & Johnson C.A. 2024. Patterns and trend analysis of rain-on-snow events using passive microwave satellite data over the Canadian Arctic Archipelago Since 1987. *Journal of Hydrometeorology 25*, 311–324, doi: 10.1175/JHM-D-22-0218.1.

Serreze M.C. & Barry R.G. 2011. Processes and impacts of Arctic amplification: a research synthesis. *Global and Planetary Change 77*, 85–96, doi: 10.1016/j.gloplacha.2011.03.004.

Serreze M.C., Gustafson J., Barrett A.P., Druckenmiller M.L., Fox S., Voveris J., Stroeve J., Sheffield B., Forbes B.C., Rasmus S., Laptander R., Brook M., Brubaker M., Temte J., McCrystall M.R. & Bartsch A. 2021. Arctic rain on snow events: bridging observations to understand environmental and livelihood impacts. *Environmental Research Letters 16*, article no. 105009, doi: 10.1088/1748-9326/ac269b.

Serreze M.C., Voveris J., Barrett A.P., Fox S., Blanken P.D. & Crawford A. 2022. Characteristics of extreme daily precipitation events over the Canadian Arctic. *International Journal of Climatology 42*, 10353–10372, doi: 10.1002/joc.7907.

Taylor A.D.M. 2005. *Inuit Qaujimajatuqangit about Population Changes and Ecology of Peary Caribou and Muskoxen on the High Arctic Islands of Nunavut*. Master's thesis, Queen's University, Kingston, ON.

Tews J., Ferguson M.A.D. & Fahrig L. 2007. Potential net effects of climate change on High Arctic Peary caribou: lessons from a spatially explicit simulation model. *Ecological Modelling 207*, 85–98, doi: 10.1016/j.ecolmodel.2007.04.011.

Tomaselli M., Kutz S., Gerlach C. & Checkley S. 2018. Local knowledge to enhance wildlife population health surveillance: conserving muskoxen and caribou in the Canadian Arctic. *Biological Conservation 217*, 337–348, doi: 10.1016/j.biocon.2017.11.010.

U.S. National Ice Center 2008. IMS Daily Northern Hemisphere Snow and Ice Analysis at 1 km, 4 km, and 24 km Resolutions. Version 1. Accessed on the internet at https://nsidc.org/data/g02156/versions/1 on 16 November 2023.

Vickers H., Malnes E. & Eckerstorfer M. 2022. A synthetic aperture radar based method for long term monitoring of seasonal snowmelt and wintertime rain-on-snow events in Svalbard. *Frontiers in Earth Science 10*, article no: 868945, doi: 10.3389/feart.2022.868945.

Voveris J. & Serreze M. 2023. A tale of two events: Arctic rain-on-snow meteorological drivers. *Annals of Glaciology 64*, 194–205, doi: 10.1017/aog.2023.25.

Walsh J., Ballinger T., Euskirchen E., Hanna E., Mård J., Overland J., Tangen H. & Vihma T. 2020. Extreme weather and climate events in northern areas: a review. *Earth-Science Reviews 209*, article no. 103324, doi: 10.1016/j.earscirev.2020.103324.

Wickström S., Jonassen M.O., Cassano J.J. & Vihma T. 2020. Present temperature, precipitation, and rain-on-snow climate in Svalbard. *Journal of Geophysical Research—Atmospheres 125*, e2019JD032155, doi: 10.1029/2019JD032155.

Wilson R.R., Bartsch A., Joly K., Reynolds J.H., Orlando A. & Loya W.M. 2013. Frequency, timing, extent, and size of winter thaw–refreeze events in Alaska 2001–2008 detected by remotely sensed microwave backscatter data. *Polar Biology 36*, 419–426, doi: 10.1007/s00300-012-1272-6.